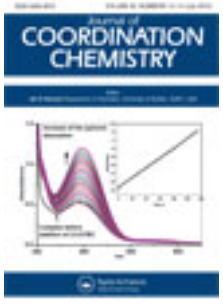

Journal of Coordination Chemistry
Publication details, including instructions for authors and subscription information:
http://www.tandfonline.com/loi/gcoo20

Syntheses, equilibrium, and structural studies of copper(II) and nickel(II) complexes with a tripodal alanine-based ligand

Ahmed Messadi [a], Aminou Mohamadou [a], Isabelle Déchamp-Olivier [a] & Laurent Dupont [a]

[a] Institut de Chimie Moléculaire de Reims, Groupe de Chimie de Coordination, CNRS UMR 7312, Université de Reims Champagne-Ardenne, Moulin de la Housse, BP 1039 - 51687 Reims cedex 2, France

Accepted author version posted online: 22 May 2012.Published online: 07 Jun 2012.

To cite this article: Ahmed Messadi, Aminou Mohamadou, Isabelle Déchamp-Olivier & Laurent Dupont (2012) Syntheses, equilibrium, and structural studies of copper(II) and nickel(II) complexes with a tripodal alanine-based ligand, Journal of Coordination Chemistry, 65:14, 2442-2458, DOI: 10.1080/00958972.2012.696107

To link to this article: http://dx.doi.org/10.1080/00958972.2012.696107

Journal of Coordination Chemistry
Vol. 65, No. 14, 20 July 2012, 2442–2458

Taylor & Francis
Taylor & Francis Group

Syntheses, equilibrium, and structural studies of copper(II) and nickel(II) complexes with a tripodal alanine-based ligand

AHMED MESSADI, AMINOU MOHAMADOU*,
ISABELLE DÉCHAMP-OLIVIER and LAURENT DUPONT

Institut de Chimie Moléculaire de Reims, Groupe de Chimie de Coordination, CNRS UMR 7312, Université de Reims Champagne-Ardenne, Moulin de la Housse, BP 1039 – 51687 Reims cedex 2, France

(*Received 26 January 2012; in final form 20 April 2012*)

A heptadentate ligand, tris[(L)-alanyl-2-carboxamidoethyl]amine (H_3trenala), has been synthesized as its tetrahydrochloride salt; its protonation constants and the stability constants of the copper(II) and nickel(II) chelates have been determined by potentiometry. Mononuclear species with protonated, neutral, or deprotonated forms of the ligand, $[Cu(H_5trenala)]^{4+}$, $[M(H_4trenala)]^{3+}$, $[M(H_3trenala)]^{2+}$, $[M(H_2trenala)]^{+}$, and [M(Htrenala)] ($M = Cu^{2+}$ and Ni^{2+}) have been detected in all cases, while only Cu^{2+} gives dinuclear $[Cu_2(H_2trenala)]^{2+}$, $[Cu_2(Htrenala)]^{2+}$, $[Cu_2(trenala)]^{+}$, and $[Cu_2(trenala)(OH)]$ species. Two dinuclear copper(II) complexes have been prepared and characterized by spectroscopic techniques (IR, UV-Vis, mass electro-spray) and thermogravimetric analysis.

Keywords: Copper(II); Nickel(II); Alanyl; Potentiometry; Stability constant

1. Introduction

The coordination chemistry of various metal centers with ligands containing carboxamide moieties has received much attention. Identification of deprotonated carboxamido *N*-coordination in bleomycin [1, 2] centers in nitrogenase [3] and nitrile hydratase [4] has raised interest in bioinorganic model studies [5–7]. For a better understanding of the physicochemical properties of complexes with ligands having pyridine-2-carboxamide, we investigated the coordination behavior of different metal ions (Co^{2+}, Ni^{2+}, Cu^{2+}, and Zn^{2+}) with: (i) hexadentate linear ligands involving two picolinamide groups and containing NH, O, or S as the heteroatom donors [8, 9]; the structural, redox, and thermodynamic properties of these complexes depend on the nature of the two heteroatoms; (ii) a potentially tripodal ligand, containing three pyridylcarbamoyl groups connected to tris(2-aminoethyl)amine which allows the characterization of mononuclear and particularly the dinuclear zinc(II) complexes [10].

In order to obtain a more complete picture of the factors influencing the electronic and stereochemical properties of these metal complexes, we report here the

*Corresponding author. Email: aminou.mohamadou@univ-reims.fr

ISSN 0095-8972 print/ISSN 1029-0389 online
http://dx.doi.org/10.1080/00958972.2012.696107

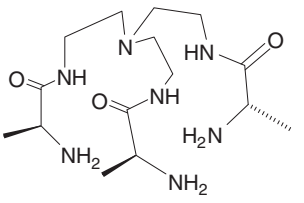

Scheme 1. Schematic representation of free ligand H_3trenala.

coordination of copper(II) and nickel(II) with a tripodal heptadentate ligand containing alanyl moieties (scheme 1). We thoroughly investigated the formation of complexes in aqueous solution as well as the preparation of solid complexes. The formation constants were determined by potentiometry. The speciation models, the stoichiometry of the species detected, and the structures for the main aqueous complexes were determined on the basis of electron paramagnetic resonance (EPR), electronic spectroscopy, and mass spectrometry. Two dinuclear copper(II) complexes have been synthesized and characterized by infrared (IR), UV-Vis, mass spectroscopy, and thermogravimetric analysis.

2. Experimental

2.1. *Reagents*

All solvents were purified by conventional procedures [11] and distilled prior to use. Chemicals commercially available (Aldrich) were used as supplied without purification.

2.2. *Synthesis*

2.2.1. Synthesis of the ligand. *Tris[(L)-alanyl-2-carboxamidoethyl]amine tetrahydrochloride tetrahydrate* (*H_3trenala $4HCl \cdot 4H_2O$*). The ligand was obtained from coupling of the carboxylate moieties using triphenylphosphite. To a solution of (L)-Boc-alanine (4.73 g, 30 mmol) in pyridine (100 mL), a solution of tris(2-aminoethyl)amine (1.46 g, 10 mmol) in pyridine (25 mL) was added dropwise under stirring at room temperature. The resulting emulsion was stirred for 60 min at 70°C. To the solution obtained, triphenylphosphite (12.33 g, 45 mmol) was added dropwise under stirring. The mixture was refluxed overnight. After cooling the reaction mixture to room temperature and removal of solvent under reduced pressure, the orange brown oil thus obtained was dissolved in chloroform (100 mL). The resulting solution was washed three times with water, three times with a saturated ammonium chloride solution, and then with brine. The organic layer was dried over Na_2SO_4 and filtered. The filtrate was roto-evaporated to give a brown viscous liquid which was taken up in ethanol (50 mL). The solution was acidified with concentrated HCl (pH $\approx$ 1.5) and the pale brown crude crystalline product which precipitated was filtered off, washed with ethanol, and dried *in vacuo*. Yield: (4.43 g, 78%). Anal. Calcd for $C_{15}H_{45}N_7O_7Cl_4$ (%): C, 31.20; H, 7.86; N, 16.98; Cl, 24.56. Found: C, 31.50; H, 7.95; N, 16.80; Cl, 25.0. ^{1}H NMR (D_2O,

250 MHz, δ_H/ppm): 1.40 (3H, d, CH_3); 4.01 (1H, q, CH); 3.35 (2H, t, CH_2); 3.55 (2H, t, CH). IR (KBr pellet, cm^{-1}): 3450 (vs, ν_{OH}); 3220–2950 (s, ν_{NH}); 2900–2800 (m, ν_{CH}); 1683 (vs, $\nu_{C=O}$); 1560 (m, ν_{CN} and δ_{NH}). MS ES+ (m/z): found 361.3, 289.2; Calcd for $[H_5trenala]^{2+}$, $[H_3trenala - alanyl(C_3H_6NO) + 2H]^+$ 361.5 and 289.4, respectively.

2.2.2. Synthesis of copper(II) complexes. For the syntheses of the copper(II) complexes (**1** and **2**), a common procedure was carried out using copper(II) perchlorate hexahydrate and H_3trenala, as described below. To a solution of the ligand tetrahydrochloride tetrahydrate (0.58 g, 1 mmol) dissolved in water (40 mL), a solution of copper(II) perchlorate hexahydrate (0.74 g, 2 mmol) in water (10 mL) was added under stirring. Solid sodium carbonate was added in small portions to the mixture with stirring until the pH reached 6.5 (**1**) or 8.5 (**2**). After stirring at room temperature for 1 h, the solution was concentrated to *ca* 20 mL on a rotovap and 20 mL of ethanol was added. A blue filtrate was then collected from the resulting solution and kept at room temperature. After a few days, blue crystalline complexes were collected by filtration, followed by washing with ice-water and ethanol, and then drying in vacuum.

Caution! Although we have experienced no problems while handling any of the substances described herein, readers are cautioned to handle these compounds as potentially explosive compounds.

2.2.2.1. *$[Cu_2(Htrenala)(OH_2)_4](ClO_4)_2$ (**1**).* Yield: (0.49 g, 65%). Anal. Calcd for $C_{15}H_{39}N_7O_7Cu_2Cl_2$ (%): C, 23.85; H, 5.20; N, 12.98; Cu, 16.82. Found: C, 23.99; H, 4.90; N, 12.71; Cu, 16.50; m.p. 208°C. IR (KBr pellet, cm^{-1}): 3400 (vs, ν_{OH}); 3205–2930 (s, ν_{NH}); 2900–2800 (m, ν_{CH}); 1620 (vs, $\nu_{C=O}$); 1090 (vs, ν_{ClO4}); 1520 (m, ν_{CN} and δ_{NH}). MS ES^+ (m/z): found 482.05 and 421.13; calcd for $[Cu_2(trenala)]^+$ and $[Cu(trenala) + 2H]^+$ 482 and 421, respectively. UV-Vis [λ_{max}, nm (ε, L $mol^{-1}cm^{-1}$)]: (solid-state), 600; (DMF solution), 600 (183).

2.2.2.2. *$[Cu_2(trenala)(OH_2)_4]ClO_4$ (**2**).* Yield: (0.39 g, 60%). Anal. Calcd for $C_{15}H_{38}N_7O_{11}Cu_2Cl$ (%): C, 27.50; H, 5.85; N, 14.97; Cu, 19.40. Found: C, 27.81; H, 5.92; N, 14.75; Cu, 19.15; m.p.: 222°C. IR (KBr pellet, cm^{-1}): 3420 (vs, ν_{OH}); 3210–2935 (s, ν_{NH}); 2900–2800 (m, ν_{CH}); 1592 (vs, $\nu_{C=O}$); 1090 (vs, ν_{ClO4}); 1520 (m, ν_{CN} and δ_{NH}). MS ES^+ (m/z): found 482.05 and 421.13; calcd for $[Cu_2(trenala)]^+$ and $[Cu(trenala) + 2H]^+$ 482 and 421, respectively. UV-Vis [λ_{max}, nm (ε, L $mol^{-1}cm^{-1}$)]: (solid-state), 558; (DMF solution), 630 (130).

2.3. *Physical measurements*

Elemental analyses (carbon, hydrogen, and nitrogen) were determined using an automatic Perkin–Elmer 2400 CHN elemental analyzer. UV-Vis spectra were recorded using a Shimadzu UV-2401-PC spectrophotometer equipped with a standard syringe sipper and a temperature-controlled cell holder TCC-240 A (equilibrium studies) and a Varian Cary 5000 spectrometer for the solid state (solid complex); the visible spectra were obtained by depositing the compound on Schleicher and Schul ash-free filter paper and the paper was used as the reference. IR spectra were obtained in KBr pellets with a Nicolet Avatar 320. ^1H NMR spectra were recorded in D_2O at room temperature with a Bruker AC 250 spectrometer. Chemical shifts (in ppm) for ^1H NMR spectra were

referenced to residual protic solvent peaks. X-band EPR spectra of the frozen solutions were recorded at 150 K using a Bruker ESP 300 spectrophotometer equipped with a Bruker E035M Gauss meter and a HP 5350B microwave frequency counter using DPPH ($g = 2.0037$) as a standard. Thermogravimetric experiments were carried out on a 2950 TA-Analyzer under nitrogen with a heating rate of $10^{\circ}C\,min^{-1}$ from room temperature to 600°C. The metal analysis was performed on an ICP AES Liberty Series II Varian apparatus and chloride was determined potentiometrically using silver nitrate.

Electrospray ionization mass spectrometry (ESI-MS) was carried out on a hybrid tandem quadrupole/time-of-flight (Q-TOF) instrument, equipped with a pneumatically assisted electrospray (Z-spray) ion source (Micromass, Manchester, UK) operated in positive mode. The electrospray potential was set to 3 kV in positive ion mode and the extraction cone voltage was varied between 30 and 90 V to obtain optimized mass spectra. Solutions of the complexes were prepared under similar conditions to the ones set out for the potentiometric study and were introduced using a syringe pump with a flow rate of $5\,\mu L\,min^{-1}$.

Peaks corresponding to the complex species were identified by analyzing their specific isotopic profile due to different Cu isotopes (e.g. ^{63}Cu, ^{65}Cu). The stoichiometries of the molecular associations were determined using the greater isotopic peak (e.g. ^{63}Cu) and further checked by simulating the different parts of the spectrum with the Isopro 3.0 software [12]. The difference between experimental and calculated m/z values was less than or equal to 0.1 unit. High-resolution mass spectra were monitored for solid compound on a Q-TOF Micromass positive ESI (CV = 30 V).

2.3.1. Potentiometric techniques. *Protometric*. Distilled and argon-bubbled water was used for preparation of all solutions. Stock solutions of metal nitrate were prepared from commercially available reagents (Fluka) of the highest purity (>99%) and were used without purification. The titrating solutions of carbonate-free NaOH and nitric acid $0.1\,mol\,L^{-1}$ were prepared from standardized molar solutions (Prolabo). All solutions were prepared with glass-distilled, de-ionized water, and degassed by argon saturation to remove all dissolved CO_2.

Protometric titrations were carried out with an automatic titrator composed of a microprocessor burette Metrohm Dosimat 665 and a pH-meter Metrohm 713 connected to a computer. The combined type "U" glass electrode used has a very low alkaline error. The titration was fully automated. All measurements were performed within a thermoregulated cell at 25°C under an argon stream to avoid dissolution of carbon dioxide. All equilibrium measurements were carried out in 25.00 mL sample volumes under magnetic stirring. The ionic strength was adjusted to 0.1 with sodium chloride. A HCl solution of exactly $10^{-2}\,mol\,L^{-1}$ was used to calibrate the electrode. The electrode slope was checked by titration with an HCl solution, and no correction was necessary in the pH range 2–12. The titrant, a carbonate-free NaOH solution (Normadose), was standardized against a $0.05\,mol\,L^{-1}$ potassium hydrogen phthalate solution by pH-potentiometry. The ionic product of water was determined under these conditions ($pK_w = 13.76$) and used in the calculations.

For a classical titration, a total of 120–150 points (volume of titrant, pH) was taken. The protonation constants of H_3trenala were determined from seven titrations. The concentrations of the ligand were $1–4 \times 10^{-3}\,mol\,L^{-1}$. In the case of the copper complexes the ligand and metal concentration ranged from 1 to $4\times10^{-3}\,mol\,L^{-1}$ with a

ratio C_L/C_M varying from 0.5 to 2. For nickel complexes the ligand concentration was equal to 2×10^{-3} mol L^{-1}, and the metal concentration varied from 1×10^{-3} to 4×10^{-3} mol L^{-1}. Thus, the ratio C_L/C_M ranges from 0.5 to 2.

Protometric computations. The protonation constants of the ligand and overall stability constants (β_{mlh}) of the metal complexes were calculated with the general computation program HYPERQUAD [13]:

$$\beta_{mlh} = \frac{[M_m L_l H_h]}{[M]^m [L]^l [H]^h},$$

$$mM + lL + hH \rightleftharpoons M_m L_l H_h,$$

(with M the metal ion, L the ligand, and H the proton, the charges are omitted). The computer program HYSS [14] was used to obtain the species distribution curves.

2.3.2. Spectroscopic studies. Spectrophotometric titrations of Cu(II) and Ni(II)-H_3trenala systems were monitored in aqueous solutions with the same concentration range as used for the potentiometric titration; an average of 40 spectra was recorded from pH 2.5 to 11.5.

Solutions for EPR study were prepared by adding appropriate volumes of the ligand and the metal solutions to obtain a [L]/[Cu(II)] ratio of 0.5, 1, and 2. The pH was then adjusted with an NaOH solution (0.1 mol L^{-1}) according to values where the maximum percentage of one species was found in the species distribution diagrams; 20% ethylene glycol was added to ensure formation of glasses. The EPR spectra were simulated using XSophe software version 1.1.4 [15].

3. Results and discussion

3.1. *Synthesis*

The new tripodal heptadentate H_3trenala containing alanyl groups is obtained *via* a single-step synthesis of the amide from tris(2-aminoethyl)amine (tren) and boc-alanine, activated by triphenylphosphite (scheme 2).

Potentiometric titration of the ligand by silver nitrate confirmed that this compound was isolated as the tetra-hydrochloride salt; four of the seven basic groups are likely to be protonated. The mass spectrum gave clear ions $[H_5\text{trenala}]^{2+}$ and $[H_3\text{trenala} - \text{alanyl}]^+$ at m/z 361.3 and 289.2, respectively.

The blue copper(II) complexes **1** and **2** were synthesized by treating an aqueous solution of the ligand hydrochloride salt and copper(II) perchlorate hexahydrate in basic conditions (pH $\approx$ 6.5 and 8.5, respectively); carbonate acts as a base to deprotonate the NH amido groups of the ligand. The variation of the copper/ligand ratios in the synthesis has no influence on the stoichiometry of the final compounds. The two complexes were recrystallized from mixed water–ethanol (1 : 1) but no suitable crystals for structure determination were obtained. All our attempts to isolate nickel(II) complexes resulted in precipitation of intractable yellowish solid.

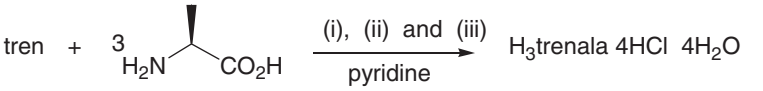

(i) 100°C, 60 min; (ii) + $P(OPh)_3$, reflux overnight; (iii) = + HCl conc in EtOH

Scheme 2. Synthetic route of H_3trenala.

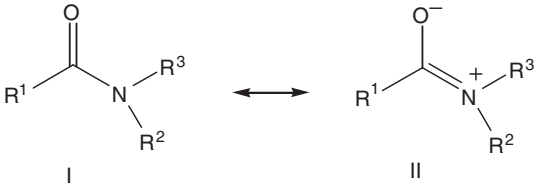

Scheme 3. Resonance of the amide.

3.2. *Spectroscopic studies*

3.2.1. Mass spectra. ESI-MS provide evidence for complex formation. The molecular peak for **1** and **2** can be identified as $[Cu_2(trenala)]^+$ and $[Cu(trenala) + 2H]^+$ at m/z 482 and 421.13.

3.2.2. IR spectra. IR spectra of these copper(II) complexes are similar to those of the ligand. We observed small shifts to lower energy for the characteristic secondary amine bands at 3210–2935 cm^{-1}, with a decrease in intensity. ClO_4^- in **1** and **2** has a strong band at *ca* 1090 cm^{-1}. H_3trenala has three amido groups and each group has resonance structures [16] shown in scheme 3; formula I predominates. Coordination through an oxygen atom increases the contribution of formula II. If coordination occurs through nitrogen, its hybridization will be sp^3 and the C=O bond will become a complete double bond with loss of the resonance energy [17].

The amide I band consists mainly of $\nu_{C=O}$, and the amide II and III bands arise from ν_{C-N} as well as from δ_{N-H}, although these modes are coupled to one another [18]. Consequently for an amide group coordinated through oxygen, the amide I band shifts to lower frequency and the amide II and III to higher frequencies. On the other hand, if amide-nitrogen coordinates, the amide I, II, III bands should shift in opposite directions. Our experimental data (see section 2) reveal that the amide bands of **1** and **2** shift in the direction expected for amide nitrogen coordination and coordination of the amide-nitrogen leads to its deprotonation.

3.2.3. Thermogravimetric analysis. The thermal stability of each new compound was probed by thermogravimetric analysis. H_3trenala shows one visible thermal step from 50°C to 150°C corresponding to the loss of four water molecules of crystallization (Obs. 13.2%, Calcd 12.5%). The destruction of the ligand starts at 150°C and continues until 370°C.

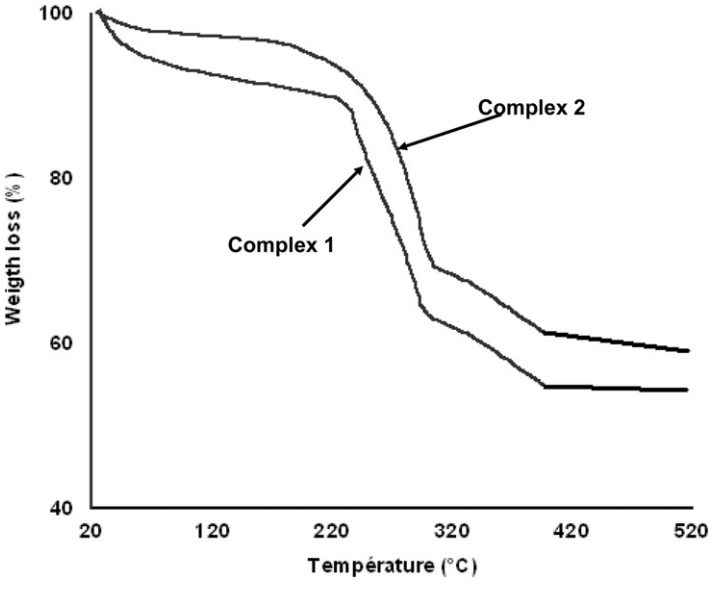

Figure 1. TGA of **1** and **2**.

In order to avoid explosion of perchlorate during the decomposition of **1** and **2**, TGA experiments were carried out under nitrogen from room temperature to 500°C. These complexes show three thermal steps, followed by a continuous weight loss until 400°C (figure 1). The first weight loss (50–220°C) corresponds to loss of four coordinated water molecules (Obs. 9.3 and 10.8%, Calcd 9.5 and 11.0 % for **1** and **2**, respectively), indicating dehydration. The second weight loss (19.3 (**1**) and 22.1 % (**2**)) from 220°C to 300°C could be assigned to loss of two alanyl moieties (C_3H_6NO) of the ligand (Calcd 19.1 (**1**), 22.0 % (**2**)). The third weight loss (9.3 (**1**) and 10.9 % (**2**)) from 300°C to 400°C corresponds to degradation of the remaining alanyl of the ligand (Calcd 9.5 (**1**), 11.0 % (**2**)). From 400°C to 500°C, no weight loss was observed. The total weight loss of 37.9 (**1**) and 43.8% (**2**) correspond to the final residue being $[Cu_2(C_6H_{16}N_4)](ClO_4)_2$ (62.5%) and $[Cu_2(C_6H_{15}N_4)]ClO_4$ (56.9%), respectively ($C_6H_{16}N_4$ or $C_6H_{15}N_4$ being di or trideprotonated tris(2-aminoethyl)amine).

The high residue percentage left without degradation in all the complexes reveals the stability of the coordination sphere around copper.

3.2.4. Electronic spectra. To investigate whether the solid state structure is retained in solution, UV-Vis spectral behavior was investigated in solution (DMF) as well as in the solid state. The overall patterns for spectra corresponding to each complex are similar. The electronic spectra for these complexes exhibit similar patterns in the 250–450 nm range, with strong bands that may be due to intra-ligand [19] and charge transfer transitions.

In the visible region a d–d band is obtained in each case. For **1**, the same spectrum is obtained in the solid state and in DMF solution. Thus, **1** exhibits a dissymmetric band with λ_{max} being 600 nm. The most significant differences are the blue shift (*ca* 72 nm) of

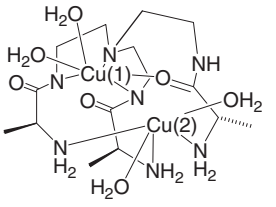

S1: $Cu(1)N_3O_3$ and $Cu(2)N_3O_2$

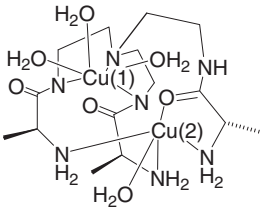

S2: $Cu(1)N_3O_3$ and $Cu(2)N_3O_2$

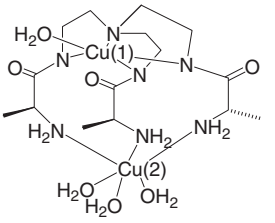

S3: $Cu(1)N_4O$ and $Cu(2)N_3O_3$

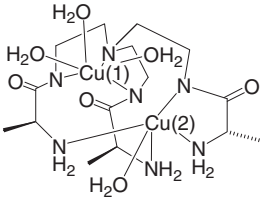

S4: $Cu(1)N_3O_3$ and $Cu(2)N_4O$

Scheme 4. Representation of the structure formulae for Cu(II) dinuclear complexes.

the λ_{max} value of **2** in DMF solution. This shift could be indicative of axial coordination by DMF substituting water or some structural rearrangement around Cu(II).

Thus, from mass, IR, UV-Vis spectral data, and thermal analysis, **1** and **2** are dinuclear compounds, in agreement with their silent EPR analysis. In these complexes, H_3trenala is doubly and triply deprotonated in **1** and **2**, respectively. Possible coordination polyhedra of these compounds can be exemplified as shown in scheme 4.

3.3. *Solution equilibria*

The affinity of H_3trenala (L) toward copper(II) and nickel(II) ions was studied in aqueous solution. The chemical model was established on the basis of potentiometric, UV-Vis spectrophotometric and mass spectrometric studies. Representative titration curves of the ligand alone and in the presence of Cu^{2+} or Ni^{2+} are depicted as $\hbar$ *versus* pH,

$$\hbar = \frac{1}{C_L}(nC_L - [H^+] + [OH^-] - C_B + C_H)$$

where $\hbar$ is the mean number of bound protons per mol of ligand, n is the number of protons in the neutral form of the ligand, C_L is the total concentration of the ligand, C_B is the concentration of the strong base added and C_H is the concentration of the strong acid initially added. Figure 2 represents the $\hbar$ variation for a solution of ligand alone and for metal-ligand solutions with the ratio $R = [L]/[M^{2+}] = 0.5$, 1 or 2 (M = Cu or Ni).

Ligand protonation constant. In ligands containing amide groups, several authors [20, 21] have shown that protonation of the amidic nitrogen is not possible ($pK_a \approx -8$) and the deprotonation of this amidic nitrogen is not observed in water ($pK_a \geq 15$). Only

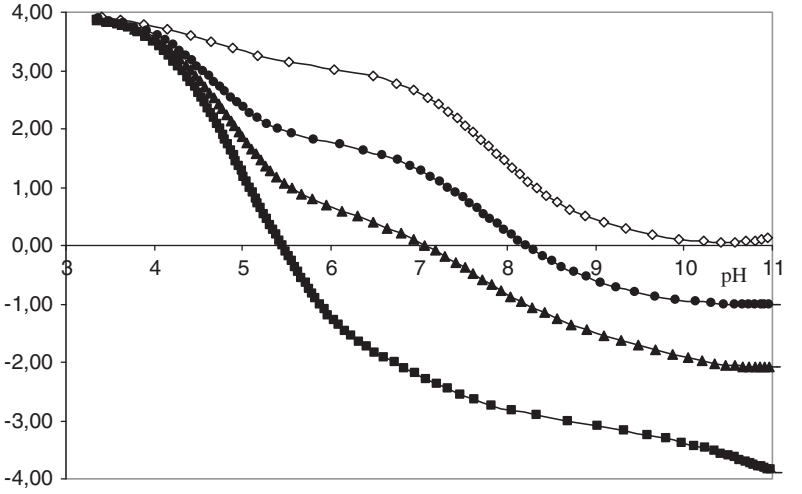

Figure 2. Average number of protons $\bar{n}$ bound per mole of H_3trenala as a function of pH Cu–H_3trenala solution (◇) ligand alone, (●) $R=2$, (▲) $R=1$, (■) $R=0.5$.

Table 1. Logarithms of equilibrium constants of H_3trenala and Cu(II) and Ni(II) complexes; $I=0.1$ mol L^{-1} (NaCl); 298 K.

	H_3trenala (L)		
log β_{011}	8.69 (1)	HL^+/L	$pK_{a4}=8.69$
log β_{012}	16.49 (1)	H_2L^{2+}/HL^+	$pK_{a3}=7.80$
log β_{013}	23.86 (1)	H_3L^{3+}/H_2L^{2+}	$pK_{a2}=7.37$
log β_{014}	28.51 (1)	H_4L^{4+}/H_3L^{3+}	$pK_{a1}=4.65$
	H3trenala – Cu^{2+}	H_3trenala – Ni^{2+}	
log β_{112}	22.15 (2)	–	
log β_{111}	17.52 (3)	13.54 (2)	
log β_{110}	11.72 (2)	6.29 (2)	
log β_{11-1}	4.25 (2)	−2.30 (3)	
log β_{11-2}	−4.42 (1)	−12.51 (3)	
log β_{21-2}	3.74 (1)	–	
log β_{21-3}	−3.40 (2)	–	
log β_{21-4}	−13.32 (2)	–	

the weak acidities of the protonated tertiary and secondary amino nitrogen atoms can be obtained from the protometric titration curves. The acid–base behavior of the ligand showed that the H_3trenala ligand possesses four protonatable nitrogen sites. All the protonation constant values are determined by titration curve refinement and reported in table 1, with the corresponding acidity constant. The pK_{a1} value corresponds to deprotonation of tertiary nitrogen whereas pK_{a2}–pK_{a4} are ascribed to successive deprotonation of the three nitrogen atoms of the primary amine. The relatively low value of pK_{a1} indicates that in H_3trenala the protons bound to tertiary nitrogen amine do not establish a hydrogen bond with oxygen of carbonyl as observed with another tripodal ligand [22].

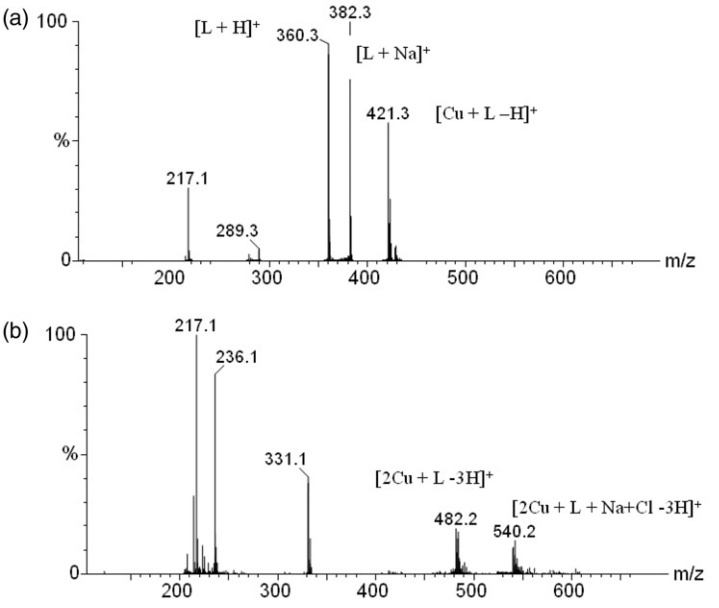

Figure 3. ESI-MS spectra from m/z 0 to 600 of Cu(II)–H_3trenala solutions with $C_L = 2\times10^{-3}$ mol L^{-1} ($L = H_3$trenala): (a) $R = 1$ and (b) $R = 0.5$.

Major complex species in aqueous solution. The protometric titrations shows that interaction of H_3trenala with Cu^{2+} is effective above pH 4 and the negative values of $\bar{n}$ above pH 6 show formation of copper(II) complexes enables deprotonation of the amide group and/or coordinated water (figure 2). For the ratio $R = 2$ and $R = 1$, $\bar{n}$ *versus* pH curves display a plateau above pH 9 with $\bar{n}$ values of -1 and -2. In both cases, these values correspond to neutralization of two protons per copper ion and the formation of $[Cu(Htrenala)]^+$. For both ratios, the ESI-MS analysis in the positive mode (figure 3) confirms the major formation of 1 : 1 species detected as proton adduct at m/z 421.3 (Cu + trenala −H). For $R = 0.5$, the absence of precipitate and the plateau observed between pH 6 and 9 for a $\bar{n}$ value of -3 corresponding to loss of 1.5 protons per Cu^{2+} are in agreement with formation of the dinuclear species $[Cu_2(trenala)]^+$ according to the reaction scheme:

$$2Cu^{2+} + H_3\text{trenala} \rightarrow [Cu_2(\text{trenala})]^+ + 3H^+.$$

This is corroborated by ESI-MS analysis which detects the formation of 2 : 1 species as proton [$m/z = 482.2$ (2Cu + L−3H)] or sodium chloride adduct [$m/z = 542.2$ (2Cu + L + Na + Cl − 3H)]. The ligand has only three deprotonatable amidic nitrogen atoms, the decrease of $\bar{n}$ beyond -3 above pH 9 can be ascribed to deprotonation of coordinated water leading to $[Cu_2(\text{trenala})(OH)]$ species.

Variable pH-UV-VIS and pH-EPR studies confirmed the results obtained from potentiometry. Figure 4 shows the variation of molar absorbance of a Cu^{2+}–H_3trenala system *versus* pH for various wavelengths. For $R = 0.5$, the absorbance of the solution below pH 4 is due to free Cu^{2+}, the maximum observed at pH 6.5 shows the formation

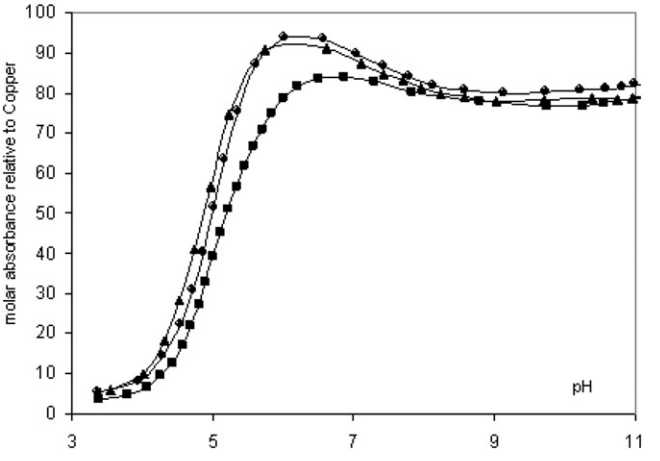

Figure 4. Molar absorbance as a function of pH of Cu–H_3trenala solutions with $C_L = 2\times10^{-3}$ mol L^{-1}: (•) $R = 2$, (▲) $R = 1$, (■) $R = 0.5$.

of another adsorbing species in addition to $[Cu_2(trenala)]^+$. At pH 6, $\hbar$ is equal to -2 (figure 2), in agreement with the release of one H^+ per copper giving thus the stoichiometry of 2 : 1 corresponding to $[Cu_2(Htrenala)]^{2+}$. The formation of dinuclear species is confirmed by EPR titrations (figure 5c), which show above pH 5 a loss of signal due to antiferromagnetic interactions between the two copper centers. For the ratio $R = 1$ and 2, whatever the pH, the EPR spectra are anisotropic and typical of axially symmetric mononuclear copper(II) complexes exhibiting tetragonal geometry.

Considering the whole results obtained on the Cu-H_3trenala system, the best chemical model corresponds to formation of $[Cu(H_3trenala)]^{2+}$, $[Cu(H_2trenala)]^+$, [Cu(Htrenala)], $[Cu_2(H_2trenala)]^{3+}$, $[Cu_2(Htrenala)]^{2+}$, $[Cu_2(trenala)]^+$, and $[Cu_2(trenala)(OH)]$. Computations were monitored taking into account protonated mononuclear species $[Cu(H_4trenala)]^{3+}$, $[Cu(H_5trenala)]^{4+}$, $[Cu(H_6trenala)]^{5+}$ and the soluble hydroxo species $[Cu(OH)]^+$ and $[Cu_2(OH)_2]^{2+}$. Formation constants of the hydroxo species were available in the compilation "critical stability constants" [23]. The stability constants for the different copper(II) complexes are given in table 1. The low values (table 1) of the estimated standard deviation of the β_{mlh} constants (< 0.95) are indicative of the validity of the model for the fitting procedure. In order to make these equilibrium constants more explicit, the distribution curves of the various species were plotted as a function of pH for $R = 2$ and 0.5 (figure 6).

For the Ni(II)–H_3trenala system, the $\hbar$ *versus* pH curve for a ratio $R = 1$ (figure 7) shows that the extra-deprotonation due to complexation is effective above pH 6. Considering the ligand in its neutral form, the $\hbar$ values above pH 10 indicate the release of two protons per ligand corresponding to formation of [Ni(Htrenala)]. The refinement of the titration curves leads us to consider successive deprotonation of 1 : 1 (Ni : L) complexes: $[Ni(H_4trenala)]^{3+}$, $[Ni(H_3trenala)]^{2+}$, $[Ni(H_2trenala)]^+$, and [Ni(Htrenala)].

The existence of 1 : 1 species was confirmed by ESI-MS (figure 8) which shows the presence of these species as were detected as proton adduct at $m/z = 416.1$. The titration of Ni–H_3trenala solution with $R < 1$ could not be investigated due to the presence of a precipitate.

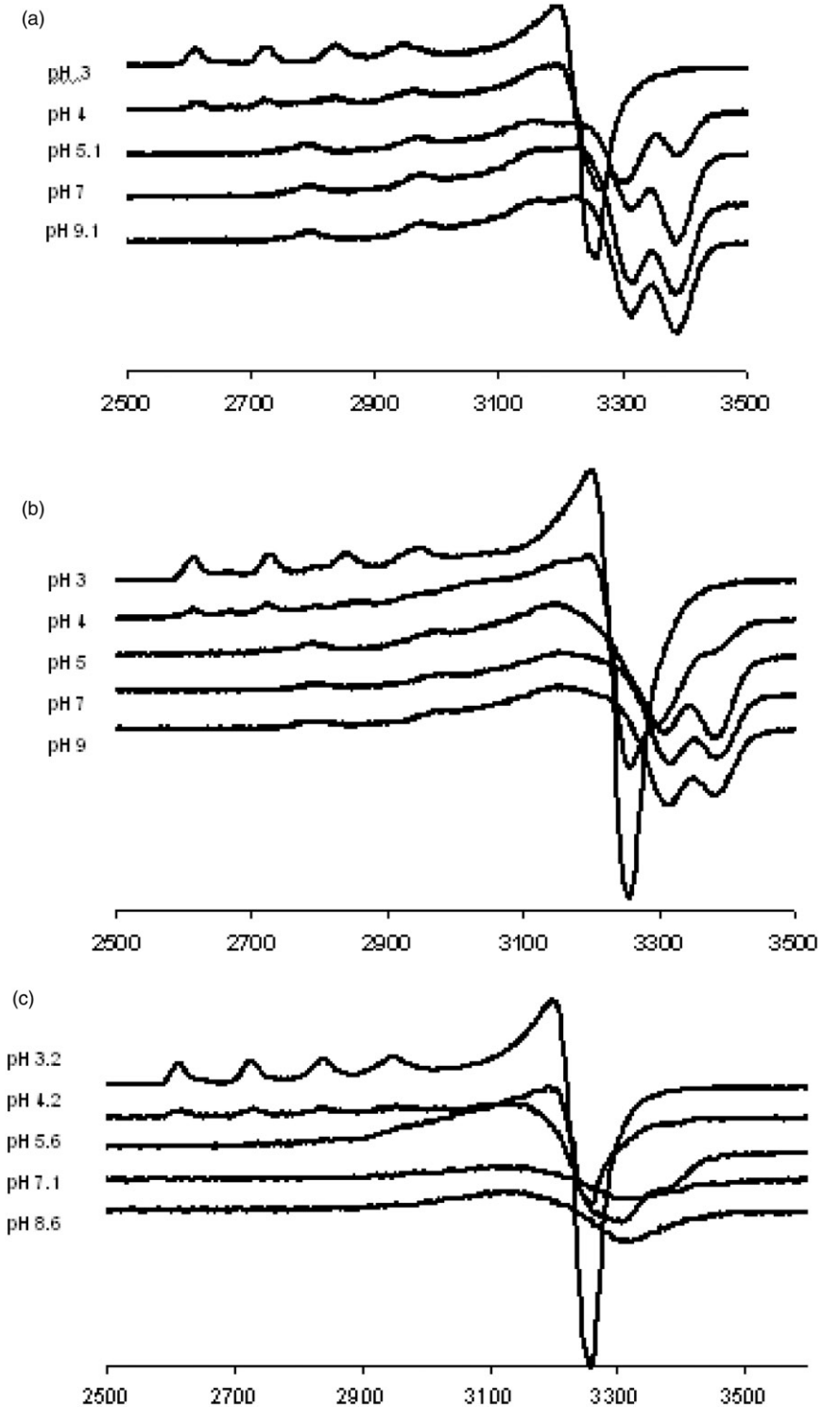

Figure 5. X-band EPR spectra recorded at 150 K of Cu(II)–H_3trenala solutions ($C_L = 2\times10^{-3}$ mol L^{-1}): (a) $R = 2$; (b) $R = 1$ and (c) $R = 0.5$.

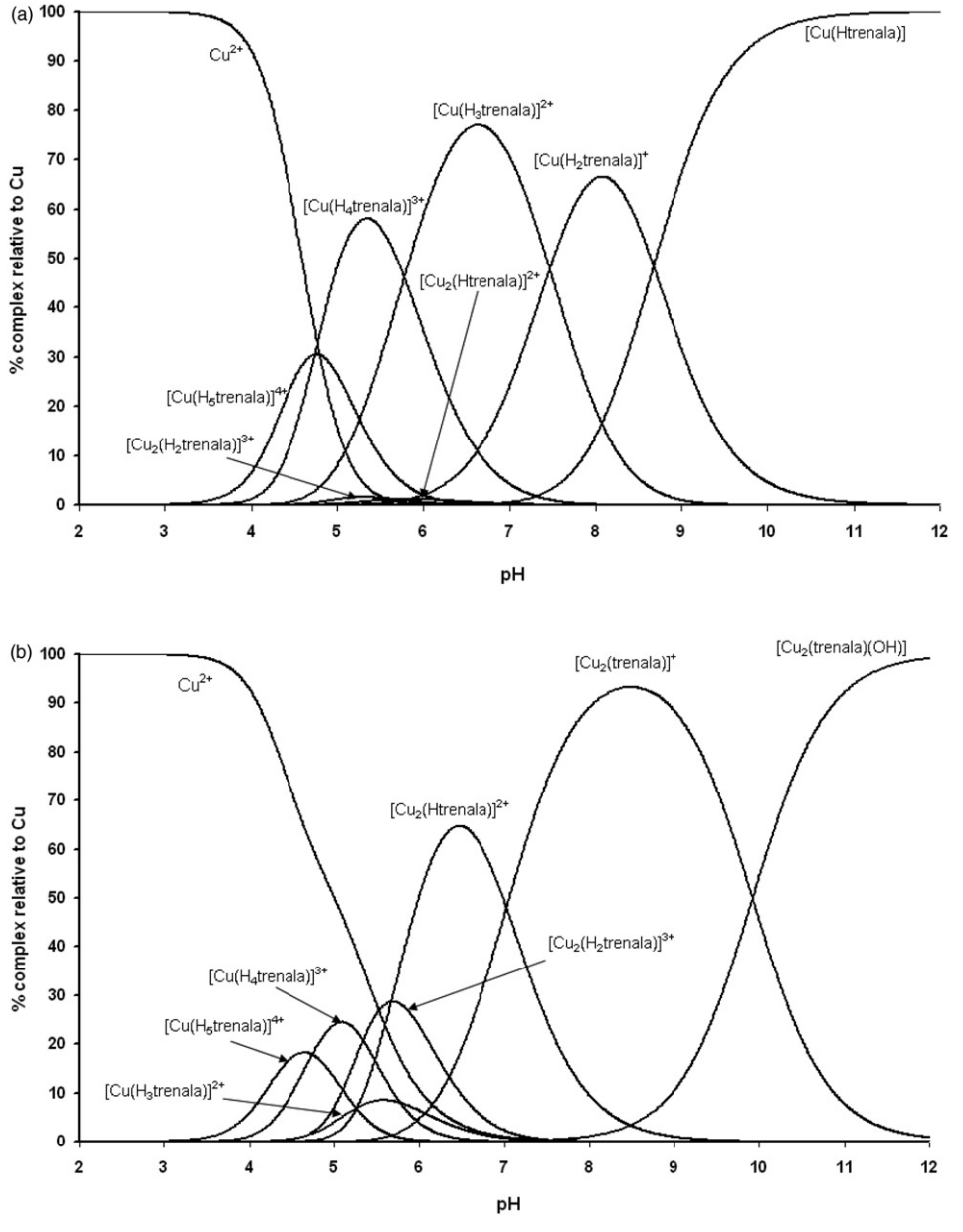

Figure 6. Distribution curves of the Cu(II)–H_3trenala system with $C_L = 2\times10^{-3}\,\mathrm{mol\,L^{-1}}$: (a) $R = 2$ and (b) $R = 0.5$.

The stability constants of the nickel(II) complexes are reported in table 1 and distribution curves given in figure 9. The difference between the successive stability constants of Ni–H_3trenala species, which are close to those of the ligand acidity constant (e.g. compare $\log\beta_{111} - \log\beta_{110}$ to pKa_2 and $\log\beta_{110} - \log\beta_{11-1}$ to pKa_3), indicate that two nitrogen atoms of the primary amine are not involved in metal

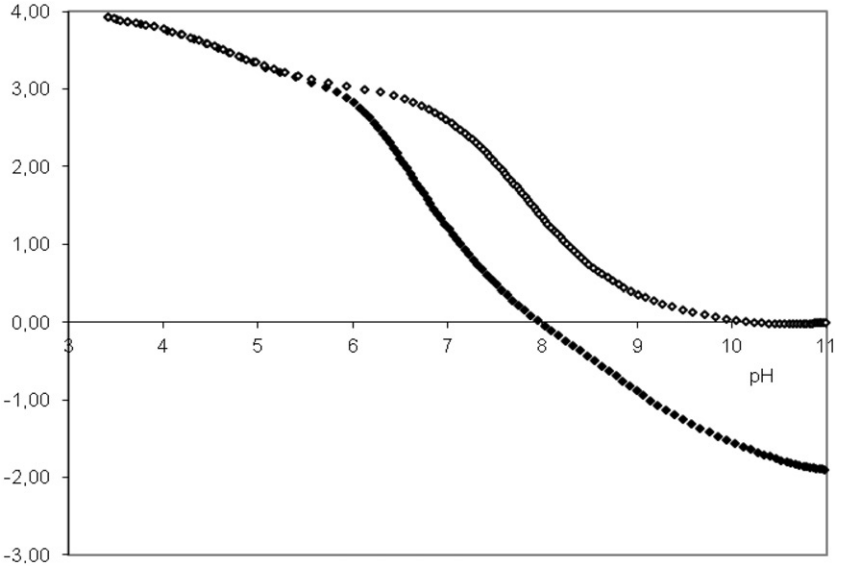

Figure 7. Average number of protons $\bar{n}$ bound per mole of H_3trenala as a function of pH Ni–H_3trenala solution (◇) ligand alone, (▲) $R = 1$.

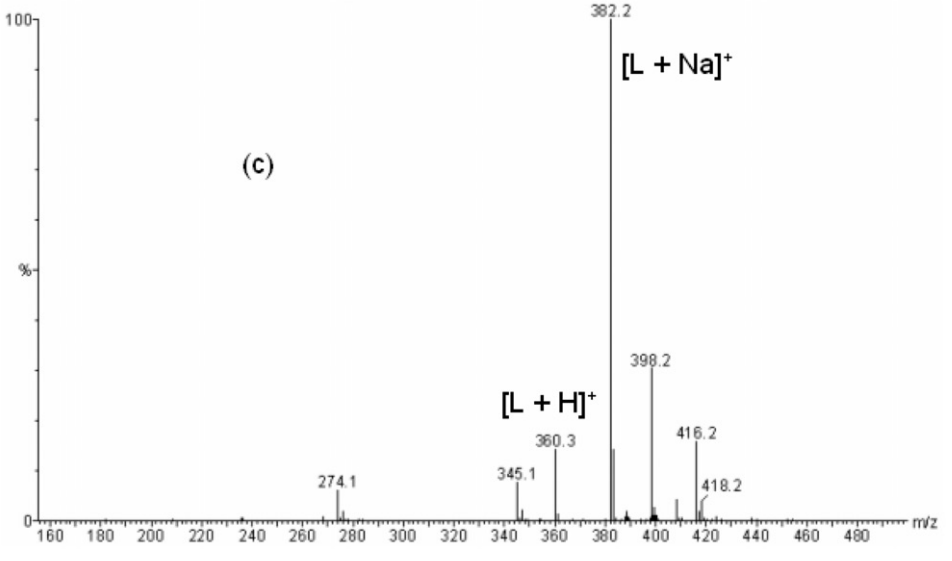

Figure 8. ESI-MS spectra from m/z 0 to 600 of Ni(II)–H_3trenala solution with $C_L = C_{Ni} = 2\times10^{-3}$ mol L^{-1} ($L = H_3$trenala).

coordination. This was corroborated by variable pH-UV-Vis studies showing the existence of only one absorbing species ($\lambda_{max} = 450$ nm) over the pH range investigated. All these 1 : 1 complexes could have the same chromophore whatever the protonation state of the ligand.

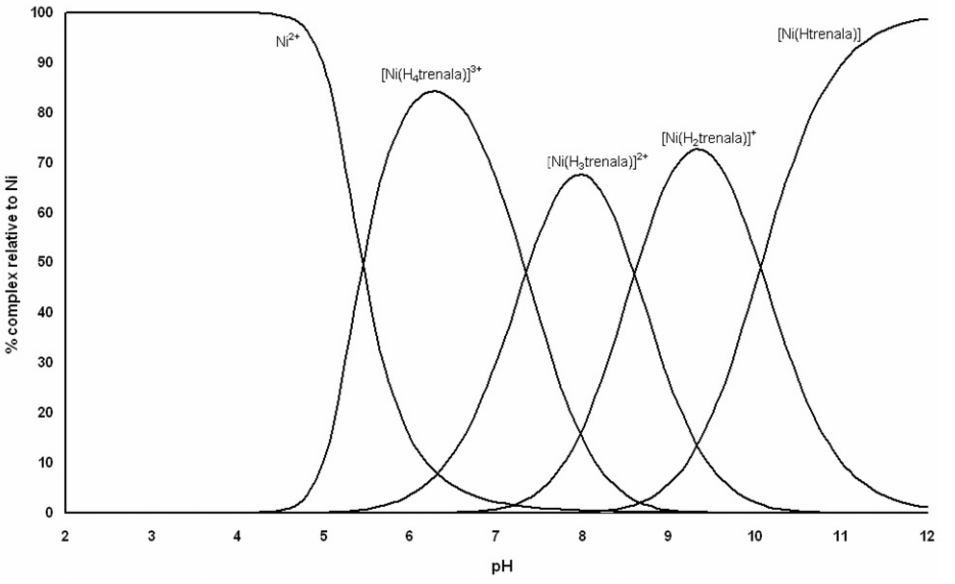

Figure 9. Distribution curves of the Ni(II)–H_3trenala system with $C_L = C_{Ni} = 2 \times 10^{-3}$ mol L^{-1}.

Table 2. Electronic and EPR data for copper(II) and nickel(II) complexes.

	λ_{max}/nm (ε L^{-1} mol^{-1} cm^{-1})	$g_{\parallel}$	$g_{\perp}$	$A_{\parallel}$
$[Cu(H_5trenala)]^{4+}$	554 (103)	2.35	2.07	140
$[Cu(H_4trenala)]^{3+}$	580 (127)			
$[Cu(H_3trenala)]^{2+}$	584 (146)			
$[Cu(H_2trenala)]^{+}$	570 (140)	2.28	2.04	161
[Cu(Htrenala)]	568 (148)			
$[Cu_2(Htrenala)]^{2+}$	605 (222)	–	–	–
$[Cu_2(trenala)]^{+}$	577 (306)	–	–	–
$[Cu_2(trenala)(OH)]$	583 (255)	–	–	–
$[Ni(H_4trenala)]^{3+}$	450 (150)	–	–	–

Metal complex structures in aqueous solution. In order to probe the solution structures of these complexes, electronic and EPR spectra have been investigated. The electronic spectra of copper complexes, computed from the spectrophotmetric titrations, show only one d–d transition in the visible region; the spectrum of $[Cu(H_5trenala)]^{4+}$, formed in a proportion less than 25%, is determined with lower accuracy. The λ_{max} value and the corresponding molar extinction coefficient for these complexes as well as their EPR parameters are given in table 2. The EPR parameters for $[Cu(H_5trenala)]^{4+}$ and $[Cu(H_4trenala)]^{3+}$ are determined from the Cu^{2+}-H_3trenala system with $R = 1$ at pH 4 (figure 5a). For both complexes, the relatively low $A_{\parallel}$ value and the high value of the empirical factor $f = g_{\parallel}/A_{\parallel}$ which exceeds 135 are indicative of a strong tetragonal distorsion [24, 25]. Above pH 5, refinement of EPR spectra of $[Cu(H_3trenala)]^{2+}$, $[Cu(H_2trenala)]^{+}$, and [Cu(Htrenala)] lead to identical parameters (figure 5a and b), indicating that these complexes could have similar coordination mode and geometry.

The larger value of $A_{\parallel}$ compared to that of $[Cu(H_5trenala)]^{4+}$ and $[Cu(H_4trenala)]^{3+}$ could be indicative of a distorted square-pyramidal geometry and strong in-plane ligand strength [26]. The symmetrical shape of the bands and the ε value of the electronic spectra as well as EPR parameters of these complexes are in agreement with those observed for copper(II) peptide complexes [27, 28].

The weak variation of λ_{max} in the electronic spectra and the same EPR parameters for the three different species show that the formation of $[Cu(H_2trenala)]^{+}$ and [Cu(Htrenala)] species from $[Cu(H_3trenala)]^{2+}$ corresponds to deprotonation of the non-coordinated amine nitrogen atoms and/or a coordinated water molecule. This is corroborated by the difference between their stability constant ($\log\beta_{110}-\log\beta_{11-1}$) and ($\log\beta_{110}-\log\beta_{11-2}$). The electronic spectra of the dinuclear species are very similar to those of mononuclear $[Cu(H_3trenala)]^{2+}$, $[Cu(H_2trenala)]^{+}$, and [Cu(Htrenala)] species, which seems to indicate that the chromophore and the geometry around the metal for these species are the same.

In the visible region, Ni–H_3trenala complexes display a broad band centered at 450 nm to the d–d transition with an extinction coefficient of *ca* 150 $L\,mol^{-1}\,cm^{-1}$, which is typical of a yellow diamagnetic Ni(II) complex and can be related to a $^1A_{1g}\rightarrow {}^1A_{2g}$, $^1B_{1g}$ transition [29] observed for other square-planar [30, 31] or square-pyramidal [32] nickel(II) complexes.

4. Conclusion

A tripodal-based alanine ligand (H_3trenala) has been synthesized and characterized. The potentiometric results reveal that only four of the seven nitrogen sites of the ligand could be protonated in aqueous solution giving $[H_7trenala]^{4+}$, $[H_6trenala]^{3+}$, $[H_5trenala]^{2+}$, and $[H_4trenala]^{+}$. The ligating properties of the ligand with metal ions, in aqueous solution, show affinity of H_3trenala toward Cu^{2+} and Ni^{2+}, forming relatively stable complexes. The potentiometric and variable pH spectrometry techniques (UV-Vis, EPR, and ESI-MS) of the metal(II)-H_3trenala systems show formation of a series of complexes with variable stoichiometry $[Cu(H_5trenala)]^{4+}$, $[M(H_4trenala)]^{3+}$, $[M(H_3trenala)]^{2+}$, $[M(H_2trenala)]^{+}$, [M(Htrenala)] ($M = Cu^{2+}$ and Ni^{2+}), $[Cu_2(Htrenala)]^{2+}$, $[Cu_2(trenala)]^{+}$, $[Cu_2(trenala)(OH)]$; the two complexes isolated in the solid state are the dinuclear $[Cu_2(Htrenala)(OH_2)_4](ClO_4)_2$ and $[Cu_2(trenala)(OH_2)_4]ClO_4$ complexes as shown by IR, EPR, and mass spectrometry measurements.

Acknowledgments

We are grateful to D. Harakat (Université de Reims, France) for mass spectroscopy analyses. We thank P. Gans, A. Sabatini and A. Vacca for free use of the Hyss program (distribution curves).

References

[1] R.M. Burger. *Struct. Bond.*, **97**, 287 (2000).
[2] S.E. Wolkenberg, D.L. Boger. *Chem. Rev.*, **102**, 2477 (2002).
[3] J.W. Peters, M.H. Stowell, M. Soltis, M.G. Finnegan, M.K. Johnson. *Biochemistry*, **36**, 1183 (1997).
[4] K.M. Kobayashi, S. Shimizu. *Curr. Opin. Chem. Biol.*, **4**, 95 (2000).
[5] D.H. Petering, R.W. Bynes, W.E. Antholine. *Chem. Biol. Interact.*, **73**, 133 (1990).
[6] J. Stubbe, J.W. Kozarich. *Chem. Rev.*, **87**, 1107 (1987).
[7] Y. Sigura, T. Takita, H. Umezawa. *Met. Ions Biol. Syst.*, **19**, 81 (1985).
[8] C. Jubert, A. Mohamadou, C. Gerard, S. Brandes, A. Tabard, J.P. Barbier. *Inorg. Chem. Commun.*, **6**, 900 (2003).
[9] C. Jubert, A. Mohamadou, C. Gerard, S. Brandes, A. Tabard, J.P. Barbier. *J. Chem. Soc., Dalton Trans.*, 2660 (2002).
[10] A. Mohamadou, C. Gerard. *J. Chem. Soc., Dalton Trans.*, 3320 (2001).
[11] D. Perrin, W.L.F. Armarego, R.D. Perrin. *Purification of Laboratory Chemicals*, 3rd Edn, Pergamon, Oxford (1988).
[12] M. Senso in Isopro 3.0 MS/MS software, Isotopic Abundance Simulator Version 3.0, National High Magnetic Field Laboratory, Sunnyvale, CA, USA.
[13] P. Gans, A. Sabatini, A. Vacca. *Talanta*, **43**, 1739 (1996).
[14] A.L. Alderighi, P. Gans, A. Ienco, D. Peters, A. Sabatini, A. Vacca. *Coord. Chem. Rev.*, **184**, 311 (1999).
[15] M. Griffin, A. Muys, C. Noble, D. Wang, C. Eldershaw, K.E. Gates, K. Burrage, G.R. Hanson. *Mol. Phys. Rep.*, **26**, 60 (1999).
[16] H. Sigel, R.B. Martin. *Chem. Rev.*, **82**, 385 (1982).
[17] J.D. Roberts, M.C. Caserio. *Basic Principles of Organic Chemistry*, p. 674, Benjamin, New York (1965).
[18] T. Miyazawa, T. Shimanouchi, S. Mizushima. *J. Chem. Phys.*, **29**, 611 (1958).
[19] B.J. Hathaway, D.E. Billing. *Coord. Chem. Rev.*, **5**, 143 (1970).
[20] R. Fersht. *J. Am. Chem. Soc.*, **93**, 3504 (1971).
[21] R.B. Martin. *J. Chem. Soc., Chem. Commun.*, 793 (1972).
[22] A. Mohamadou, C. Gérard. *J. Chem. Soc., Dalton Trans.*, 3320 (2001).
[23] Standard Reference Database 46 in Critically Selected Stability Constants, version 5 (1995). <Webook.nist.gov>.
[24] U. Sakaguchi, A.W. Addison. *J. Chem. Soc., Dalton Trans.*, 600 (1979).
[25] J. Gouteron, S. Jeannin, Y. Jeannin, J. Livage, C. Sanchez. *Inorg. Chem.*, **23**, 3387 (1984).
[26] R. Fersht. *J. Am. Chem. Soc.*, **93**, 3504 (1971).
[27] I. Sovago, D. Sanna, A. Dessi, K. Varnagy, G. Micera. *J. Inorg. Biochem.*, **63**, 99 (1996).
[28] N.V. Nagy, T. Szabo-Planka, G. Tircso, R. Kiraly, Z. Arkosi, A. Rockenbauer, E. Brucher. *J. Inorg. Biochem.*, **98**, 1655 (2004).
[29] D.J. MacDonald. *Inorg. Chem.*, **6**, 2269 (1967).
[30] L. Fabbrizzi, L. Montagna, A. Poggi, T.A. Kaden, L.C. Siegfried. *J. Chem. Soc., Dalton Trans.*, 2631 (1987).
[31] A. Urfer, T.A. Kaden. *Helv. Chim. Acta*, **77**, 23 (1994).
[32] O. Atakol, H. Nazir, C. Arici, S. Durmus, I. Svoboda, H. Fuess. *Inorg. Chim. Acta*, **342**, 295 (2003).